Scientia Iranica A (2012) 19 (1), 20–26

Sharif University of Technology

Scientia Iranica

Transactions A: Civil Engineering

www.sciencedirect.com

Mechanical properties of precast reinforced concrete slab tracks on non-ballasted foundations

M. Madhkhan [a,*], M. Entezam [b], M.E. Torki [c]

[a] *Department of Civil Engineering, Isfahan University of Technology, Isfahan, P.O. Box 8415683111, Iran*

[b] *Civil group, Department of Engineering, Bou-Ali Sina University, Hamedan, P.O. Box 651744161, Iran*

[c] *Department of Civil Engineering, Sharif University of Technology, Tehran, P.O. Box 1136511155, Iran*

Received 3 January 2011; revised 27 September 2011; accepted 19 November 2011

KEYWORDS

Slab track;
Precast concrete;
Non-ballasted foundations;
Optimum slab width;
Full-size slabs;
FEM analysis.

Abstract This article deals with the mechanical properties of steel-reinforced concrete precast slab tracks on non-ballasted elasto-plastic foundations. To work out the spanning behavior of slab tracks, a FEM analysis was executed for discrete and continuous systems. At first, full-size slabs without foundation including solid and hollow-core specimens (with 30% weight reduction) were tested under centric static (monotonic) line loads, and load–deflection curves were extracted. Then, FEM results for zero foundation stiffness were verified with those of experiments, which were in good agreement. Original results include the effects of several parameters on the cracking load, ultimate load, and energy absorption of slabs placed on elasto-plastic foundations including the slab width, concrete tensile strength and load factor. Analyses revealed that mechanical properties in hollow-core sections are not so different from those in solid ones, and thus hollow-core sections are more efficient because of significant weight reduction.

1. Introduction

The application of non-ballasted railways, especially in tunnels and bridges, has been extended widely because of reducing the height of railways, reducing maintenance and total costs, increasing the service life of the railway, facilitating higher train velocities, and increasing the lateral strength of the railway [1,2]. Non-ballasted track systems can be constructed in two basic ways: in-situ and precast. For a long time, greater attention has been directed towards precast systems for many reasons including very high quality and rapidity of construction and more trustworthiness of mix design [3].

The study of reinforced concrete slabs, either alone or placed on elastic foundations, has received increasing research. Among those available, is the work done by Falkner and Teutsch, who tested concrete slabs on foundations made of rubber and cork, by applying monotonic loads to the center point [4]. They found satisfactory agreement between the load–deflection curves obtained from experiment and those from finite-element analysis. Charles et al. analyzed slab tracks by modeling them as concrete slabs on elastic foundations using *ABAQUS* finite-element models [5]. They could finally figure out the effect of foundation stiffness, distance between fasteners and slab width on the maximum deflection and maximum stress developed in the slab. Considering the mechanical properties of slab tracks, Esveld suggested placing reinforcement at the top and bottom of the section, in order to undergo maximum tension [6]. The use of *Expanded Poly-Styrene (EPS)* under slab tracks in high-velocity railways was proposed by the same researcher, in order to reduce the dead weight of the system and, finally, to minimize the cost of stabilizing the foundation soil [7]. Zwarthoed et al. used 1% reinforcement to design slab tracks [8]. They deduced that this reinforcement percentage is sufficient to resist the applicable loads for foundations with stabilized and improved (high-quality) soil. A number of parametric studies on the mechanical properties of slab tracks on non-ballasted foundations have been worked out in the Iranian Ministry of Routes and Traffic [9]. The results expressed that the foundation stiffness (known as *Foundation Modulus*) has the most significant effect on all parameters including internal forces, stresses and displacements. It was

* Corresponding author. Tel.: +98 311 3913851.
E-mail address: madhkhan@cc.iut.ac.ir (M. Madhkhan).

1026-3098 © 2012 Sharif University of Technology. Production and hosting by Elsevier B.V. Open access under CC BY-NC-ND license.
Peer review under responsibility of Sharif University of Technology.

doi:10.1016/j.scient.2011.11.037

Production and hosting by Elsevier

also gathered that the properties as the moment of inertia of the rails do not markedly influence those parameters, but lead to more homogeneous distribution of loads on the slab. The design criteria for the vertical vibration of ballast-less slab track systems were assessed by Steenbergen et al. [10]. They used the classic beam-on-elastic-foundation model to evaluate the vibrations induced on the system by high-speed trains, and demonstrated that for high frequencies, increasing slab stiffness is the best way to control vertical vibrations, while for low frequencies, improving the sub-system soil is preferable [10]. Wanming et al. predicted the ground-induced vibrations of slab tracks by using an interactive train-track-ground model. They deduced that the interaction between the rail and the wheel caused by track irregularities is significantly effective on ground acceleration and less effective on its displacement. For frequencies above 40 Hz, ground vibrations induced in ballast-less systems were found to be much higher than those in ballasted tracks [11]. A 3D multi-body finite boundary element was used by Galvín et al. to study the vibration in ballast-less slab tracks due to High-Speed Trains (HST). They studied three types of load: quasi-static excitations (forces generated by moving loads), parametric excitations due to discrete supports of the rails, and those due to wheel and rail roughness and track unevenness. They also showed how effective a floating track would be to strictly reduce vibration in surface tracks [12]. An analytical model was developed for predicting the ground vibration caused by moving trams on slab tracks by Real et al. This model was developed, based on the wave equation, and was solved in the frequency domain by means of the Fourier transformation. Effects of harmonic and static loads and vibrations, due to loads distributed by different axles, were taken into account in this research [13].

To the best of the authors' knowledge, work on the mechanical properties of reinforced concrete slab tracks on non-ballasted foundations is meager. In the present work, attention is focused on the case of using steel reinforcement in slab tracks.

2. Research methodology

At first, solid and hollow-core full-scale precast slab tracks were made to extract load–deflection curves. The second stage of the article contains parametric studies including the effects of different factors on the mechanical properties of precast slab tracks, such as cracking and ultimate loads, and energy absorption. This stage was aimed at evaluating the efficiency of hollow-core slab tracks to find out the extent to which weight reduction (by almost 30%) changes the mechanical properties, and whether the design becomes more economic in hollow-core sections. Since it is not convenient to make real models for slab tracks on elastic foundations at the laboratory, FEM models were made for this purpose based on the models defined by Barros and Figueiras [14]. To ensure the accuracy of FEM analyses, results corresponding to zero foundation stiffness were compared to those obtained from experiments, and were in very good concurrence. Finally, the real behavior of slab tracks on elastic foundations, before and after cracking, was studied by applying monotonic loads in FEM models. The results can be used as a benchmark.

3. Spanning behavior

In order to distinguish the practical loading scheme on slab tracks, as well as avoid superfluous calculations, the spanning behavior of slab tracks must be evaluated at first. To this end, the

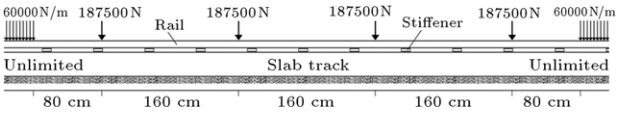

Figure 1: The loads applied to the system considering the dynamic effect.

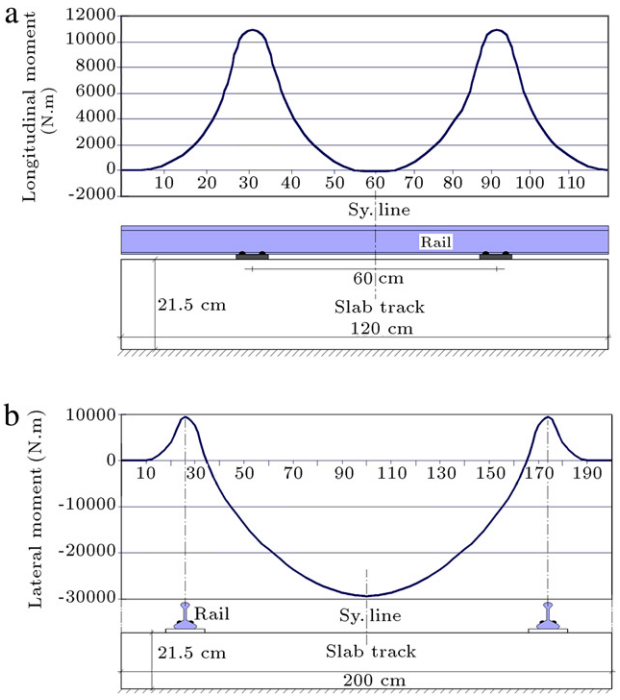

Figure 2: (a) Longitudinal, and (b) lateral moment distribution of moments in a slab track with $k_s = 50$ MN/m^3 and 2.5 m width.

distribution and magnitudes of positive and negative moments along and across the slab, and positions of the beginning and propagation of cracks were investigated. To do so, the width, length and thickness of slabs were considered as 2.5, 1.2 m, and 215 mm, respectively. The 2.5 m width was obtained as the optimum width, for which the absolute amounts of maximum positive and negative moments are equal. The distance between fasteners was taken 600 mm [5,14,15]. The *Shell* element with 6 degrees of freedom at each node was used to model the slabs; A 3D *Beam* element was used to model the rails, and springs with nonlinear behavior were used for modeling the fasteners. The loads consisted of dead and live loads, considering the impact induced by moving trains, lateral loads on curves, and longitudinal forces caused by the braking and acceleration of trains, all calculated or taken in accordance with the *UIC* code [16]. To calculate the dead load, the volumetric mass of concrete was considered 2400 kg/m^3. The loads, due to the braking and acceleration of trains, are equivalent to 1/7 times the weight of the train. Also, the lateral load applied on the railway was obtained as 38.3 kN [13].

Considering the impact influence, the most critical loading pattern, according to Ref. [17], is shown in Figure 1. In the models, the elasticity modulus and Poisson ratio were taken as 20 GPa and 0.17 for concrete, and 200 GPa and 0.3 for steel rails, respectively. The stiffness of fasteners was considered to be 40 kN/mm, and the distance between them was taken as 600 mm. The foundation modulus was taken to be 50 MN/m^3 [5]. The maximum moments and deflections occur under concentrated wheel loads. Figure 2 demonstrates longitudinal and lateral moments under the loading pattern

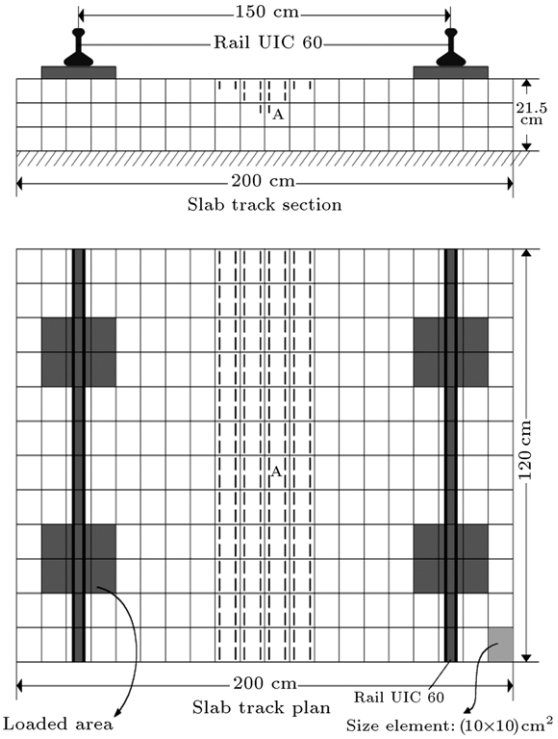

(a) Initial cracking on the middle of the upper face.

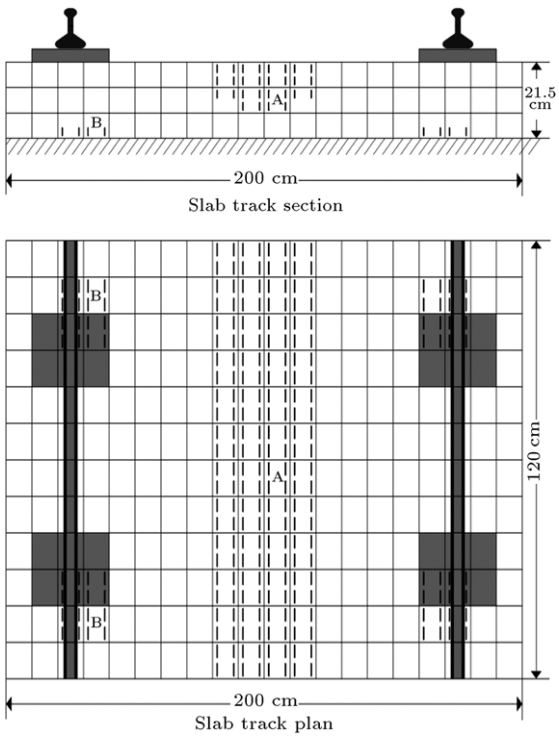

(b) Development of tensile cracks and lateral cracking initiation under the load points.

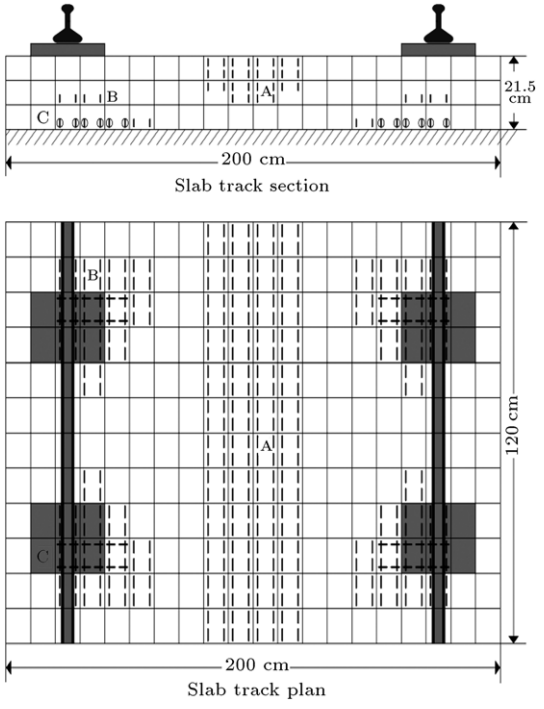

(c) Further development of lateral cracks.

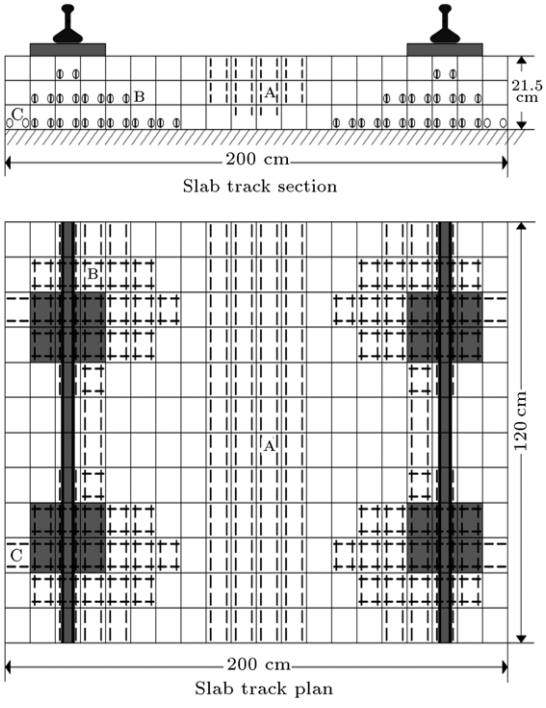

(d) Further development of lateral cracks in zone C.

Figure 3: Stages of cracking in discrete systems.

of Figure 1. It can be obviously seen that lateral moments are greater than longitudinal moments. Further analyses proved that the spanning behavior remains one-way in inelastic zones, i.e., after cracking initiation. The cracking pattern in discrete and continuous systems is shown in Figures 3 and 4. Therefore, both discrete and continuous systems have one-way spanning behavior, and thus slab tracks can be precast instead of made in situ. For design purposes, minimum reinforcement is required for the longitudinal direction, and reinforcement should be calculated only for lateral moments.

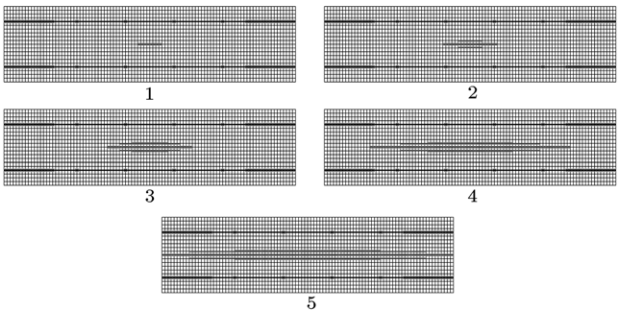

Figure 4: Stages of cracking in continuous systems.

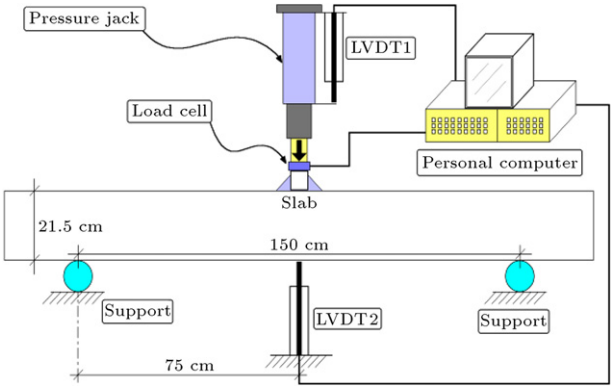

Figure 5: The setup of the bending test with centric load.

4. Experimental procedure

In order to study the mechanical properties of reinforced concrete slabs, 22 cylindrical specimens with 150 mm diameter and 300 mm height were made for compressive strength, and 2 precast slabs with $2 \times 1.2 \times 0.215$ m dimensions were produced in the *Deesman Prefabrication Factory* in Isfahan for final loading tests. One of the slab tracks was solid and the other was hollow-core with 30% weight reduction. The thickness in all models was considered to be 215 mm, which is almost equal to the 200 mm thickness put forward in [9]. The steel reinforcement was designed according to *ACI318-99* [18]. All specimens were cured for two days in a steam tunnel with 60 °C temperature.

4.1. Compressive strength

The average cylindrical compressive strength of all specimens was 50.8 MPa, with a standard deviation of 0.8 MPa.

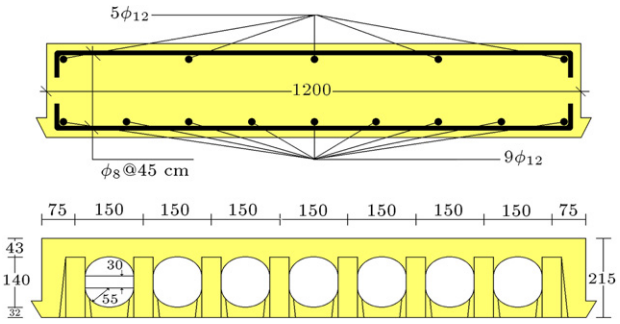

Figure 7: Details of solid and hollow-core cross sections.

4.2. Load vs. deflection curves

As stated in Section 3, slab tracks have one-way spanning behavior. On the other hand, slab tracks with 1.5 m width are devoid of negative moment. Thus, 1.5 m is the critical amount of slab width (this is why experimental specimens had 1.5 m width). Using displacement control, the slabs were put under monotonic load until fracture, according to the idea put forward by Moeen and Nemgeer stated in UIC [16]. The bending test setup is shown in Figure 5, and the fractured specimen is shown in Figure 6. Also, the details of solid and hollow-core slab cross sections are shown in Figure 7.

The required reinforcement for the slabs was calculated using the moment obtained from FEM analysis. Thus, for the slab with 1.2 m width and 215 mm thickness, 9φ12 was used as the bottom reinforcement, according to *ACI318-99*. Since the positive moment is small, we can use the minimum reinforcement set forth in *ACI*, i.e 5φ12 at the top. Figure 8 shows the load–deflection curves for slab tracks reinforced with steel bars. The values of cracking and ultimate loads for the solid specimen were $P_{cr} = 106$ kN, $P_{ult} = 246.75$ kN, and those for the hollow-core specimen were $P_{cr} = 71.6$ kN, $P_{ult} = 239.25$ kN. It can be obviously seen that the solid specimen has a greater ultimate load, more ductility and energy absorption. However, the elastic zones in the two types of specimen are coincident up to a large extent, i.e. up to 3 mm deflection. Using the load combination put forward in *AASHTO* [19], the factored load applied on the fasteners will be obtained as 157 kN, which is much lower than the load corresponding to the 30 mm deflection. Therefore, the same design may be used for hollow-core sections.

5. Theoretical modeling

At first, the material properties are explained as follows:

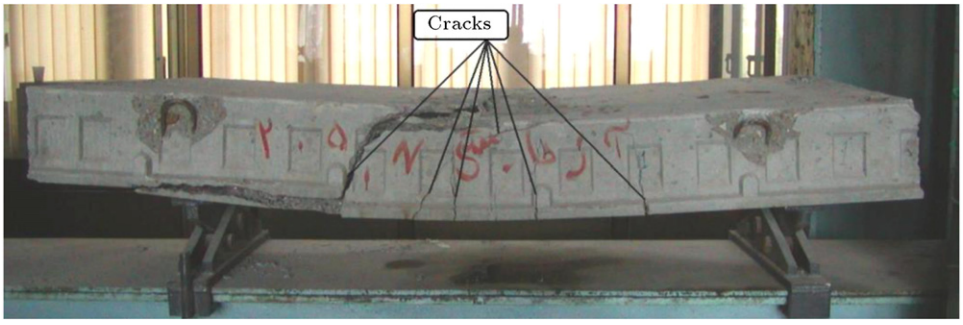

Figure 6: Reinforced slabs after fracture.

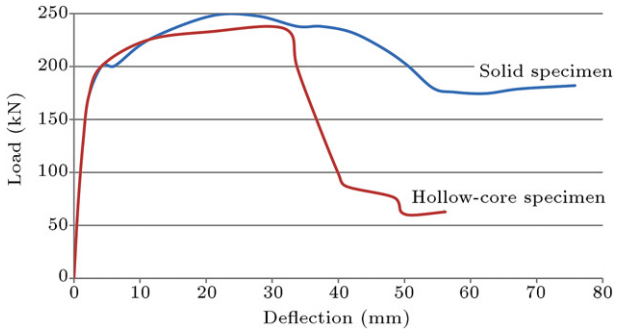

Figure 8: Load–deflection curves of slabs reinforced with steel bars.

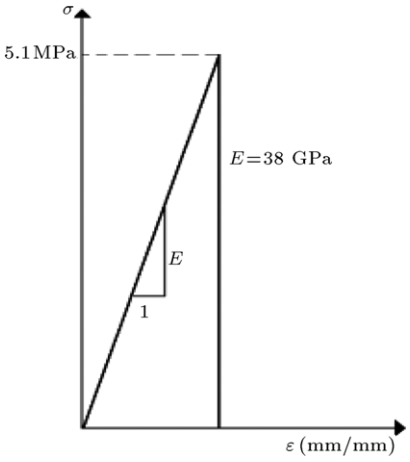

Figure 9: The tensile stress–strain model used in the analyses for plain concrete.

5.1. Concrete

5.1.1. Compressive stress–strain curve

To define the stress–stress pattern of concrete, Eq. (1) was used [14]:

$$\sigma = \frac{E_c \varepsilon}{1 + (\varepsilon/\varepsilon_0)^2}, \tag{1}$$

where σ is the stress, ε is the strain, E_c is the concrete Young's modulus, and ε_0 is the strain corresponding to maximum stress. According to Timoshenko's relation, we can use Eq. (2) for ε_0 [20]:

$$\varepsilon_0 = 2f_c'/E_c. \tag{2}$$

To make sure of the correctness of the stress–strain model, we consider f_c' as the average compressive strength of all reinforced cylindrical 150 × 300 mm specimens, i.e. 58 MPa. With this value, ε_0 will be approximately 0.003 [21].

5.1.2. Tensile stress–strain curve

Since the models proposed by Barros and Figueiras are similar to the models defined in the present research, the simplified tensile stress–strain relation shown in Figure 9 was used, except that the cracking stress was used based on experimental outcomes instead of that proposed by Barros and Figueiras [14]. As seen in Figure 9, plain concrete is supposed to damage immediately after initial cracking.

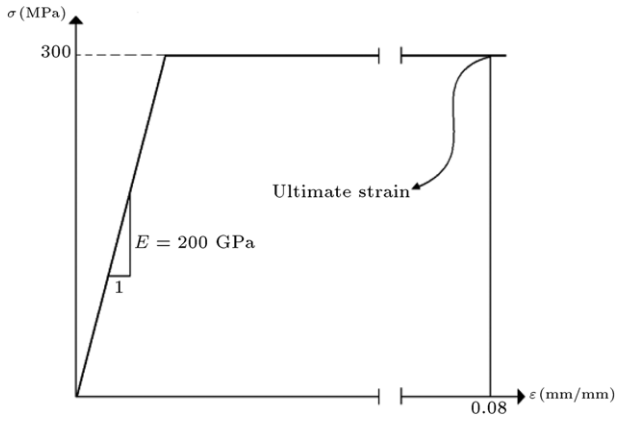

Figure 10: Tensile stress–strain curve for steel bars.

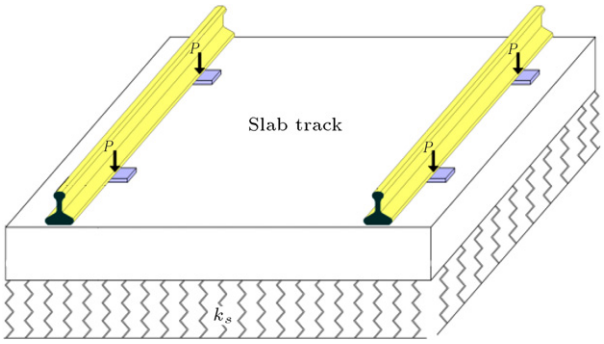

Figure 11: The schematic model of discrete systems on foundation.

5.2. Steel bars

The tensile stress–strain curve for steel bars is shown in Figure 10. The corresponding element in the models was the *Link* element.

5.3. Slab track foundation

The schematic model of the slab *on foundation* is shown in Figure 11. The concrete slabs were modeled using the *Solid* element to extract the load–deflection curves, and both *Solid* and *Shell* elements (with 6 degrees of freedom at each node) to obtain the cracking moments and elastic moments under service loads. The foundations were modeled using the *Combin* element. The dimensions of FEM slab tracks were identical to those of experimental specimens.

The foundation considered by Barros and Figueiras was cork, whose mechanical behavior is shown in Figure 12 [14]. The same model was used for the foundations in this research. In Figure 12, P and a are the forces and displacements of the foundation, respectively.

6. Results and discussion

The load–deflection curve for the slab reinforced with steel bars is shown in Figures 13 and 14 for solid and hollow-core sections, respectively. The effect of k_s on the load–deflection of solid and hollow-core slabs with 2.5 m width reinforced with steel bars is shown in Figures 15–18. The following results can be drawn.

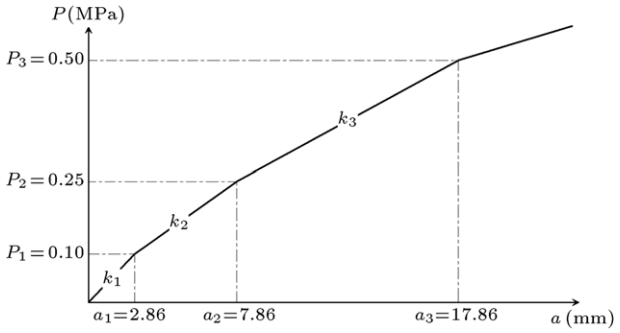

Figure 12: Mechanical behavior of the foundation.

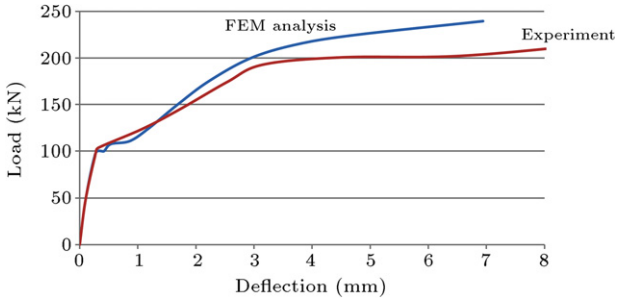

Figure 13: Comparison of FEM and experimental load–deflection curves of the reinforced *solid* slab.

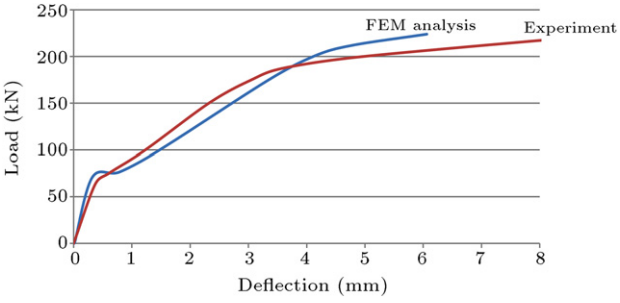

Figure 14: Comparison of FEM and experimental load–deflection curves of the reinforced *hollow-core* slab.

6.1. Load–deflection curves for slabs without foundation

Figures 13 and 14 show that the mean values of the cracking load for solid and hollow-core sections obtained from the experiment were 106 and 71.6 kN, respectively. The corresponding values from FEM analysis were 108 and 73 kN, respectively. Thus, the agreement between the two results is satisfactory and the defined models are quite realistic.

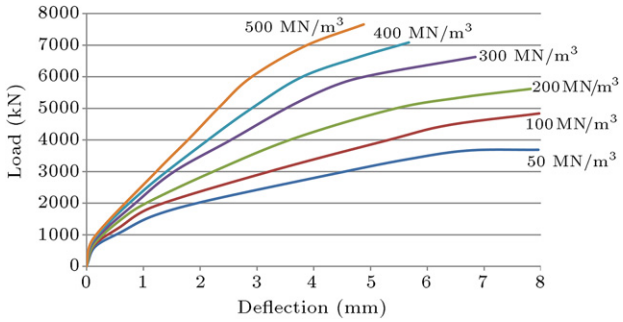

Figure 16: Effect of k_s on the load–deflection of solid slabs reinforced with steel bars with 2.5 m width.

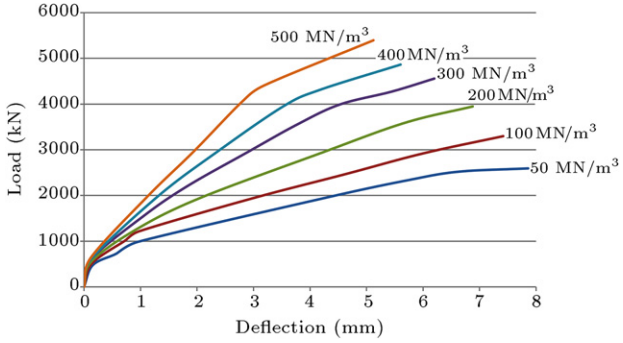

Figure 17: Effect of k_s on the load–deflection of hollow-core slabs reinforced with steel bars with 2.5 m width.

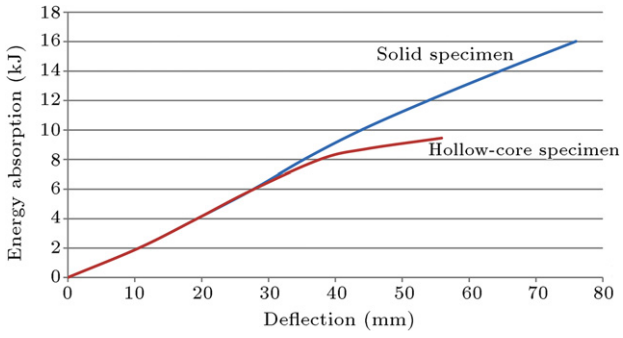

Figure 18: Comparison between the energy absorption of reinforced solid and hollow-core specimens for *zero* foundation stiffness.

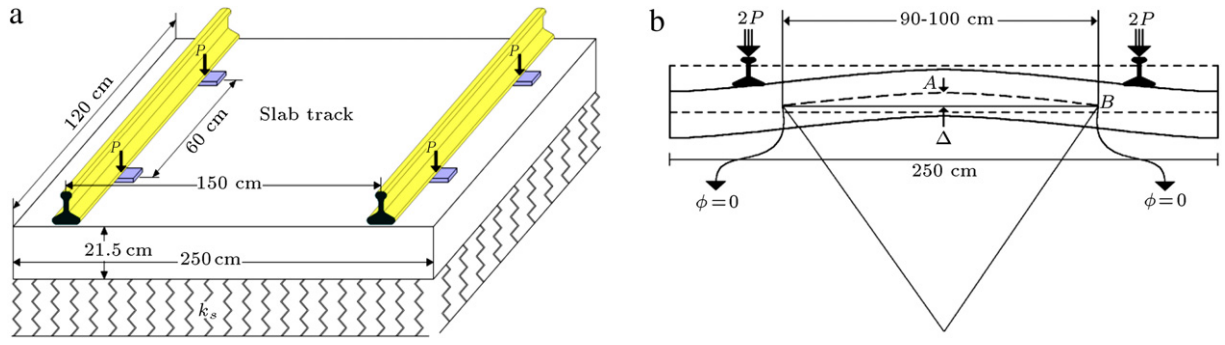

Figure 15: The models relating to the effect of k_s on the load–deflection curve. (a) Dimensions used in the model; and (b) deflection considered in the curves.

6.2. Load–deflection curves for slabs on foundation

As seen in Figure 15b, the loads are applied on four points. The dimensions used in the models concerning the effect of k_s are shown in Figure 15a. The slab width was considered as 2.5 m, since previous analyses proved that the optimum width, for which the positive and negative moments are almost equal, is 2.5 m. $\phi = 0$ signifies the contraflection point where the moment is zero. The deflection considered in the curves is the (average) difference between the deflection(s) of contraflection point(s) with that of the center point. The load–deflection curves for slabs reinforced with steel bars are shown in Figures 16 and 17. These two figures express that increasing k_s will cause both the cracking and ultimate load to increase, but decreases the ductility, i.e. the area beneath the load–deflection curve. Also, the cracking load, ultimate load, and ductility of solid slabs are greater than those of hollow-core slabs. However, the elastic zones in the two types of specimen are to a large extent coincident. For instance, as shown in Figure 18, the elastic zones for $k_s = 0$ are coincident up to 30 mm. The case in Figure 18 is the critical case for design purposes, since the deflection decreases with k_s. On the other hand, using the load combination put forward in *AASHTO* [19], the factored load applied on the fasteners will be obtained as 157 kN, which is much smaller than the load corresponding to the 30 mm deflection. Thus, this deflection never occurs under typical loads exerted on slab tracks by trains. Therefore, both types of slab track suffice for design purposes [8,17,19]. In this case, hollow-core sections are more cost-effective, since their weight is around two thirds the weight of the solid section.

7. Conclusions

In the present article, the mechanical properties of slab tracks reinforced with steel bars were evaluated. At first, the true spanning behavior of slab tracks under the applied loads was distinguished by working out the finite-element analysis of discrete and continuous slab tracks; it was figured out that slab tracks have a one-way spanning behavior. To assure the real behavior of FEM models, full-size precast slabs were made and tested under monotonic line loads to assess the mechanical properties of specimens without foundation, and were compared with FEM results for zero foundation stiffness. In the main FEM analyses, realistic models were made to study the effects of several parameters on the cracking and ultimate loads of solid and hollow-core specimens. To extract the load–deflection curves, monotonic loads were applied to the models until fracture. It was observed from the analyses that solid specimens have higher cracking and ultimate load capacities and higher energy absorption. However, load–deflection curves were coincident up to the linear limit in which the maximum deflection is 3 mm, which is much larger than the deflection induced by loads exerted by trains. Thus, the use of hollow-core slabs is more efficacious, because they weigh about 30% less than solid slabs.

References

[1] Esveld, C. "Slab track: a competitive solution", In *Rail International*, Schienen der Welt, June (1999).
[2] Esveld, C., *Recent Developments in Slab Track*, Publication of the Department of Civil Engineering, Section of Roads and Railways, May, Delft University of Technology, Netherlands, pp. 81–86 (2003).
[3] Iran Railway Development Consultant Engineers, *Types of non-ballasted railway systems* Railway of Islamic Republic of Iran, Ministry of Routes and Transport, 1998
[4] Falkner, H. and Teutsch, M., *Comparative Investigations of Plain and Steel Fibre Reinforced Industrial Ground Slabs*, 102, Institute fur Baustoffe, Massivbau und brandschutz 70 (1993).
[5] Charles, W., Schwartz, D. and Tayabji, *Analysis of Concrete Slab Track System*, University of Maryland, Australia, pp. 159–178 (2000).
[6] Esveld, C. "Developments in high-speed track design", *Structures for High-Speed Railway Transportation-IABSE Symposium*, Antwerp, pp. 27–29 (2003).
[7] Esveld, C. and Markine, V. "Use of expanded polystyrene (EPS) sub-base in railway track design", *Proceedings van de Wegbouwkundige Werkdagen*, pp. 473–484 (2002).
[8] Zwarthoed, J.M., Markine, V. and Esveld, C. "Slab track design: flexural stiffness versus soil improvement", In *Rail-Tech. Europe*, Utrecht, ISSN 0169-9288 CD-ROM, pp. 1–22, 3–5 April (2001).
[9] Iran Railway Development Consultant Engineers, *Design of different non-ballasted railway systems* Railway of Islamic Republic of Iran, Ministry of Routes and Transport (2002)
[10] Steenbergen, M.J.M.M., Metrikine, A.V. and Esveld, C. "Assessment of design parameters of a slab track railway system from a dynamic viewpoint", *Journal of Sound and Vibration*, 306, pp. 361–371 (2007).
[11] Wanming, Z., Zhenxing, H. and Xiaolin, S. "Prediction of high-speed train induced ground vibration based on train-track-ground system model", *Journal of Earthquake Engineering and Engineering Vibration*, 9, pp. 545–554 (2010).
[12] Galvín, P., Romero, A. and Domínguez, J. "Vibrations induced by HST passage on ballast and non-ballast tracks", *Journal of Soil Dynamics and Earthquake Engineering*, 30, pp. 862–873 (2010).
[13] Real, J., Martínez, P., Montalbána, L. and Villanueva, A. "Modeling vibrations caused by tram movement on slab track line", *Journal of Mathematical and Computer Modeling*, 54, pp. 280–291 (2011).
[14] Barros, J.A.O. and Figueiras, J.A. "Model for the analysis of steel fibre reinforced concrete slabs on grade", *Journal of Computers and Structures*, Pergamon, 79, pp. 97–106 (2001).
[15] Esveld, C. *Developments Modern Railway Track*, MRT-Productions, Zaltbommel, ISBN: 90-800324-3-3, www.esveld.com (2001).
[16] UIC, The Railways—An Indispensable Part of the European Transport System, Paris (1993)
[17] Profillidis, V. "The mechanical behavior of the railroad tie", *ASCE Journal of the Structural Engineering Division* (1995).
[18] *Building Code Requirements for Structural Concrete and Commentary*, American Concrete Institute, Farmington Hills, USA, ACI 318-99 (1999).
[19] *Standard Specifications for Highway Bridges,* American Association of State Highway and Transportation Officials (AASHTO), Washington, DC (2002)
[20] Maidl, B., Stahlfaserbeton, E. and Verlag, S. "Fiber Reinforced Concrete", In *für Architektur und Technische Wissenschaften*, Berlin (1991).
[21] Ding, Y. and Wolfgang, K. "Compressive stress–strain relationship of steel fibre-reinforced concrete at early age", *Cement and Concrete Research*, 30, pp. 1573–1579 (2000).

Morteza Madhkhan is Assistant Professor in the Department of Civil Engineering at Isfahan University of Technology (IUT), in Iran from where he received his B.S. degree. He received his M.S. degree from Sharif University of Technology, Iran, and his Ph.D. degree from the University of Lille, France. His research interests include high-strength and high-performance concrete, roller compacted concrete (RCC), fiber reinforced concrete, optimum design of structures and seismic design of precast concrete structures.

Majid Entezam is an M.S. degree graduate in Civil Engineering. He received his B.S. and M.S. degrees from Bou-Ali Sina University, in Iran, and performed his experiments at Isfahan University of Technology, Iran. His research interests include fiber-reinforced and high-performance concrete.

Mohammad Ebrahim Torki Harchegani is a M.S. degree graduate of Civil Engineering. He received his B.S. degree from Isfahan University of Technology, Iran, and his M.S. degree from Sharif University of Technology, Iran. His research interests include functionally graded materials, prestressed concrete structures, Roller Compacted Concrete (RCC) pavements and high performance concrete.